Water Air Soil Pollut (2021) 232: 311
https://doi.org/10.1007/s11270-021-05260-7

Zinc Removal Mechanisms with Recycled Lignocellulose: from Fruit Residual to Biosorbent then Soil Conditioner

Birol Kayranli · Oguzhan Gok · Turan Yilmaz · Gulden Gok · Hakan Celebi · Ismail Yigit Seckin · Demet Kalat

Received: 22 March 2021 / Accepted: 2 July 2021 / Published online: 20 July 2021

Abstract This study aims to remove zinc by using banana peel from an aqueous medium. The peel was a lignocellulosic adsorbent and characterized by FTIR spectra, SEM–EDS images, and elemental analysis. The effect of contact time, pH, and adsorbent dosage on the sequestration of zinc was observed. The sorption process of zinc was well described with the pseudo–second-order kinetic and Langmuir isotherm model. The rate-limiting step to the adsorption process was determined by applying the intra-particle diffusion model. The removal mechanism is that ion exchange, electrostatic interaction, complex formation, physical adsorption, and precipitation carried out in cooperation with the banana peel functional groups and zinc ion in many ways. FTIR analysis demonstrates that the surface carboxylic/hydroxyl functional groups of banana peel play a key role in the adsorption of zinc ions. The results showed that banana peel, a locally available fruit residual, is an efficient and eco-friendly adsorbent to reduce Zn^{2+}. The usage of banana peel as an adsorbent for the sequestering of zinc from water ensures both the technical advantage and cost-effectiveness of the sustainable environmental management concept and zero waste strategy. Furthermore, the value-added products containing organic compounds and zinc can be used efficiently as a soil conditioner.

Keywords Zinc · Lignocellulosic adsorbent · Soil conditioner · Removal mechanism · Zero waste strategy

B. Kayranli (✉)
Graduate School of Natural and Applied Science, Department of Environmental Science, Gazi University, Ankara, Turkey
e-mail: bkayranli@gazi.edu.tr; bkayranli@hotmail.co.uk

O. Gok · G. Gok · H. Celebi
Department of Environmental Engineering, Aksaray University, Aksaray, Turkey

T. Yilmaz · I. Y. Seckin · D. Kalat
Department of Environmental Engineering, Cukurova University, Adana, Turkey

1 Introduction

Zinc is a transition metal, produced 10.5 Mt in all the world in 2020, and mostly used in pesticides and chemical fertilizer in agriculture activity and in medicine, mining, smelting, battery producing, paints, and pigments in the industrial sector because of its having strong binding capability (Li et al., 2021a, Li et al., 2021b). The excessive production and usage of zinc cause the eco-toxicological risk when discharging to nature without applying any purification process (Xu et al., 2017). Zinc and its compounds can accumulate into the food chain and aquatics, resulting in toxic living things. Zinc exposure beyond the allowable levels brings about many health problems, lung, bladder, breast, respiratory systems cancer, immune systems, gastrointestinal distress, and neurological signs

(Jagaba et al., 2020). Therefore, the World Health Organization (WHO) listed the permissible level of 5.0 mg/L in drinking water.

On the other hand, zinc is an essential micronutrient and cofactor that supports the body and immune system, and biological processes need zinc especially for cell growth (Lonergan & Skaar, 2019). The availability of zinc in the soil prevents loss of yields and retarded growth. The complex structure form makes it difficult to uptake nutrients from the plants. However, these complexes can be converted into simple forms by the number of soil microorganisms. The availability of organics in soil supports nutrient ability and mobility, soil humidity, and microorganism activity. It is critical to increasing the organic compound in soil due to increased water holding capacity, microorganism activity, nutrients, and mineral availability (Dimkpa et al., 2020).

Wastewater including zinc has to be applied to some treatment processes to reduce the metal concentrations in discharge criteria before giving off the receiving body. One of the most used treatment methods for the removal of zinc is adsorption. The process provides high efficiency, flexibility, ease in operation, and cost-effectiveness compared to other conventional methods (Saeed et al., 2021). Fruit residuals are considered wastes and used to remove heavy metals from an aqueous solution such as potato, orange, grapefruit, banana peels, seed shells, tea leaf, agricultural by-product, and coffee husks (Baloo et al., 2021; Costa et al., 2021) due to its cost and readily available adsorbents.

The use of the fruit residuals as end-products reduces its disposal cost and protects the environment. Recycling and reusing fruit and vegetable residuals is an important strategy in the economy to protect natural resources and effectively use recyclable materials (Sanka et al., 2020). Banana is a mostly consumed fruit with a global production of 116 million tons in 2019 (FAO, 2020). The banana fruit comprises bioactive compounds, phenolic constituents, carotenoids, vitamins, and dietary fiber. The weight of banana peel is ranging 40–30% out of the total fruit weight; however, it is usually treated as a waste product with disposed at dumping side, burning, and composting, resulting in producing green gases emission such as methane and carbon dioxide (Sial et al., 2019). Approximately 35 million tons of banana peel are produced in the food industry, and humans consume it on yearly bases worldwide. The peels are composed of organic matter such as holocellulose and lignin, and minerals such as potassium, calcium, sodium, iron, and manganese (Liew et al., 2017). Banana peel contains a large amount of potassium, important to enhance optimal plant growth, and acts as an activator of protein synthesis, sugar transport, N and C metabolism, and photosynthesis. It also affects yield formation, improves crop quality, and is critical for cell growth (Oosterhuis et al., 2014). Potassium plays a critical role in regulating cell osmotic pressure and balancing the cations and anions in the cytoplasm due to strong mobility in plants (Hu et al., 2016). These peels can be used in various food applications and sorption processes as an adsorbent. However, no one considered a comprehensive environmental protection approach for both metal reduction and use of the final product. The end-product includes valuable organics and metals. Therefore, it is necessary to describe the potential usage of the value-added products for a sustainable environmental protection approach. The usage of this by-product as a value-added product is a benefit for the long-term sustainability of the banana industry.

The treatment of zinc from wastewater prior to giving the environment is crucial for the protection and safety of the ecosystem. Similarly, the recovery of the organic material and waste minimization is one of the advantages of using fruit residuals as an adsorbent in the treatment process (Jagaba et al., 2021). The chemical fertilizer is used highly in the farming activity that brings about deterioration of soil hypoxia, alkalinity, microbial, and water balances. The limited fertile land and water sources are needed to develop organic amendments for sustainable agricultural development and protect the environment (Sauer, 2018). The improvement of physicochemical properties, chemical composition, and nutrient contents in the soil is supplied by applying organic soil amendments. Soil conditioners contain organic materials to release nutrients and hold water in soils and have positive effects on the soil's biological, physical, or chemical nature. Another usage area of the soil conditioner is as a plant growth medium. There is a growing interest in compostable materials used in farming areas and materials made from natural replenishable resources due to ecological concerns (Wang et al., 2020). When zinc wastes are removed by banana peels and recovered properly, they

can be utilized for organic soil conditioners and plant growth mediums.

Previous researches focused on fruit residuals' adsorption capacity and zinc removal efficiency rather than removal mechanism and beneficial usage of the final products. For that reason, the present study aims to evaluate the removal mechanism of zinc and adsorption capacity and the beneficial use of end-product as soil amendments. The possible removal mechanism of the banana peel was defined with the help of sorbent compounds, FTIR spectra, and SEM images. The use of end-product obtained in the treatment process was evaluated from the perspective of zero waste strategy.

2 Materials and Methods

2.1 Materials and Reagents

The banana peel was collected from Aksaray University central eating hall, and then the white part of the inside was carefully removed until the yellow outer skin remains. The yellow skin was dried out in the oven (Memmert UN750, Germany) at 105 °C for more than 24 h. The dried skin was cleaned with deionized water, obtained a Direct-Q® 3, 5, 8 Laboratory Water Purification Systems, Merck KGaA, Darmstadt, Millipore, Sigma system, until the water turned clear. After the peel cleaning and dried again, turned into the flour with a blender and sieved through No.5 size meshes and protected for further use.

The zinc form of $ZnCl_2$ having 96% purity and the analytical grade was supplied from Merck KGaA Chemistry, Turkey. The solution (stock 1000 mg/L) was prepared using exactly 2.09 g $ZnCl_2$ dissolved into 1000 mL pure water, and the desired concentration of Zn was diluted for further study. The solution pH, measured with a pH 510 Eutec pH meter, was adjusted to 6.0 using 0.1 mol L^{-1} HCl or 0.1 mol L^{-1} NH_4OH. All other reagents were supplied from Sigma-Aldrich Chemie Germany in this study.

2.2 Analytical Methods

After the pre-fixed contact time, Zn^{2+} concentration was carried out by using Thermo Scientific X-SERIES 2 model ICP-MS, and FTIR spectra were recorded using a Thermo Scientific-Nicolet IS20 with a spectral resolution of 4 cm^{-1} was used to define the active groups on the surface of the peel (see Fig. 1). A Hitachi-SU 1510 scanning electron microscopy was used for morphological observations of the peel sample (see Fig. 2). Origin 9.0 program (Origin Lab, USA) was used for all of the figures. The precision of the experimental data for kinetic and equilibrium studies was carried out in duplicate with a mean ± SD.

2.3 Batch Studies

The batch studies performed a 1.0 g banana peel dosage in a 100 mL glass conical flask under the

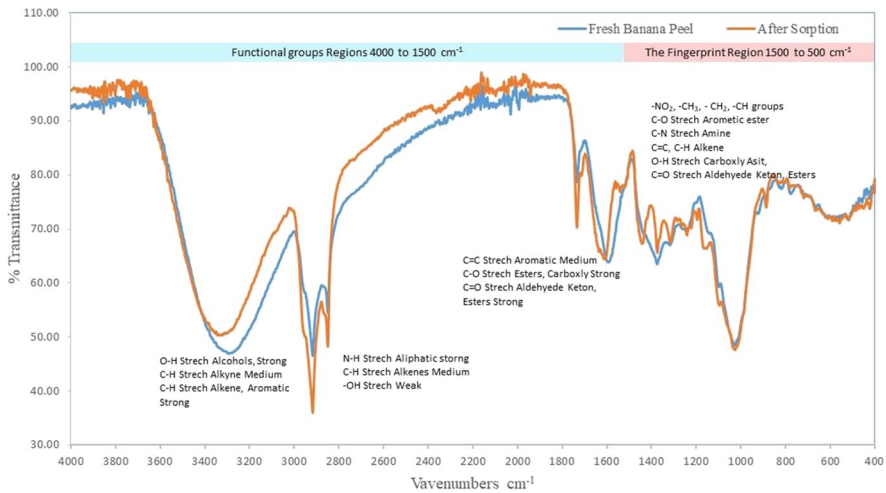

Fig. 1 Three adsorbent FTIR spectra and functional groups

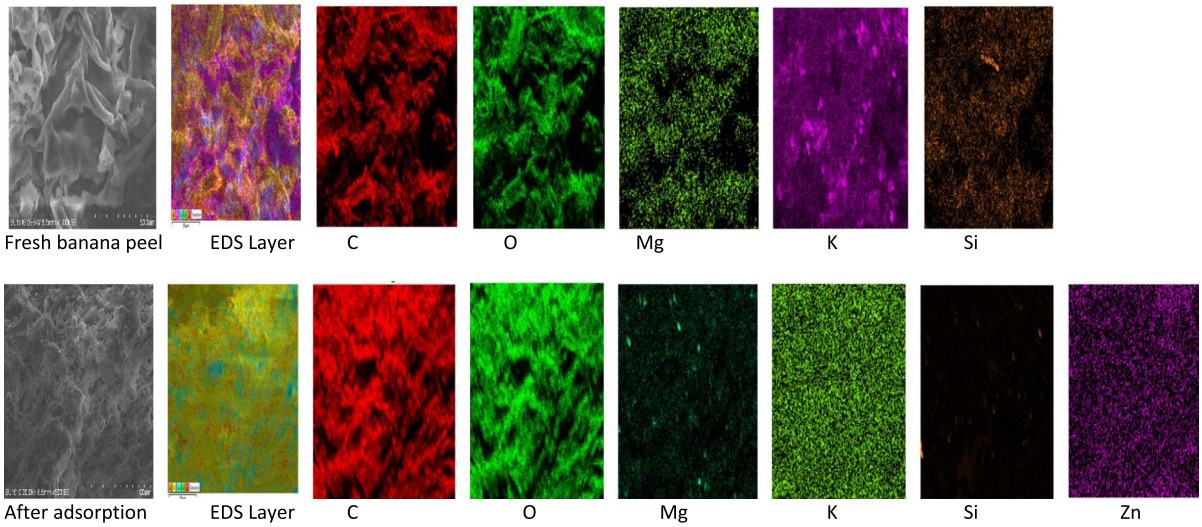

Fig. 2 SEM–EDS images of biosorbent fresh and after adsorption

initial Zn^{2+} concentration of 100 mg/L at room temperature. The flask was shaken by a ZHICHENG analytical model thermal shaker at 150 rpm for 45 min. The Zn^{2+} ion reduced amount (qe) was calculated by using the equations given below:

$$\mathrm{qe} = \frac{V\left(C_\mathrm{i} - C_\mathrm{e}\right)}{W} \tag{1}$$

qe is the amount of zinc captured from a solution (mg/g), C_i and C_e are the initial and final concentrations (mg/L), V is the volume (L), and W is the mass of peel (g). The studies were done in duplicate to provide reproducibility, reliability, and precision of the data.

2.4 Kinetic Studies

To evaluate the adsorption process and mechanism of Zn^{2+}, the Elovich, the Lagergren pseudo–first-order and second-order model (Ho & McKay, 2003), and the intra-particle model (Weber & Morris, 1963) were applied. The models' linear forms are demonstrated in Table 1. Also, the intra-particle diffusion was thought to express the sorption step of Zn^{2+} ions by adsorbents in the process.

2.5 Equilibrium Studies

To optimize the design and understand the interaction for the sorption system, it is crucial to set the most proper correlation for equilibrium (Parab & Sudersanan, 2010). Several adsorption isotherms have been aped for adsorption data: Langmuir (Langmuir, 1918), Freundlich (Freundlich, 1906), and D-R (Dubinin & Radushkevich, 1947). The equations of these isotherm models are seen in Table 1.

2.6 Adsorption Isotherm Validity

The error analysis methods, the sum of absolute errors, Marquardt's percent standard deviation, and the normalized standard deviation were applied to the experiment data's validity to determine the best fitting isotherms equation except for coefficient constant (R^2). The linearized form of equations is given in Table 1.

Table 1 Isotherm and kinetic parameters for the adsorption of Zn^{2+}

Isotherms	Parameter	Coeff.	Kinetic	Parameter	Coeff.
Freundlich	K_F	119.93	Pseudo-first order	q_e	10.06
	1/n	0.9095	$\ln(q_e - q_t) = \ln q_e - k_1 t$	k_{1p}	0.088
	R^2	0.993		R^2	0.9284
$\log q_e = \log K_F + \frac{1}{n}\log C_e$	MPSD	49.85	$\mathrm{ARE} = \frac{100}{N}\sum_{i=1}^{N}\left\lvert\frac{q_e^{exp}-q_e^{cal}}{q_e^{exp}}\right\rvert_i$	MPSD	25.96
	NSD	38.61		NSD	72.48
	ARE	33.73		ARE	87.048
Langmiur					
Type(I)	qm	322.58	Pseudo-second order	q_{me}	14.77
	KL	0.008	$\frac{t}{q_t} = \frac{1}{k_2 q_e^2} + \frac{t}{q_e}$	K_{2p}	0.0021
	RL	0.539		R^2	0.9643
$\frac{C_e}{q_e} = \frac{1}{q_{max} K_L} + \frac{C_e}{q_{max}}$	R^2	0.3984	$\mathrm{MPSD} = 100\sqrt{\frac{1}{N-p}\sum_{i=1}^{N}\left(\frac{q_{ei}^{exp}-q_{ei}^{cal}}{q_{ei}^{exp}}\right)^2}$	MPSD	13.39
	MPSD	73.39		NSD	69.064
$R_L = \frac{1}{1 + C_i K_L}$	NSD	56.84		ARE	78.28
	ARE	49.91			
	qm	92.59		k_p	9.3925
	KL	0.033	Intra-particle Diffusion	R^2	0.6562
Type(II)	RL	0.228	$q_t = k_p\sqrt{t} + C$	MPSD	894.0
	R^2	0.992		NSD	774.23
$\frac{1}{q_e} = \frac{1}{q_{max} K_L C_e} + \frac{1}{q_{max}}$	MPSD	67.78	$\mathrm{NSD} = 100\sqrt{\frac{1}{N-1}\sum_{i=1}^{N}\left[\frac{q_t^{exp}-q_t^{cal}}{q_t^{exp}}\right]_i^2}$	ARE	701.85
	NSD	52.50			
	ARE	43.00			
	qm	26.16			
	β	0.0103			
Dubinin–Radushkevich	ε	6.967			
	R^2	0.6345			
$\ln q_e = \ln q_m - \beta\varepsilon^2$	MPSD	399.62			
	NSD	309.55			
	ARE	227.23			

3 Result and Discussion

3.1 Characterization of Adsorbents

Banana peel is composed of mostly lignin, cellulose, hemicellulose, and minerals due to organic residuals. The chemical composition of the peel is as follows: 21.40% hemicellulose 18.06% cellulose, 16.45% lignin, 1.4% crude protein, 10.56% cured fiber, 4.5% ash.

The adsorption mechanism can be explained to understand and determine the surface active sites and groups. The FTIR spectra of the biosorbent were scanned in the range of 450–4000 cm^{-1}, and the result is illustrated in Fig. 1. The adsorbent peaks on the spectra showed the complexity of the sorbents. As seen in Fig. 1, the peak at 3293 cm^{-1}, the largest band, indicates many hydroxyl groups (-OH) and carboxyl groups (C-H) resulting from lignin, cellulose, and hemicellulose on a banana peel. The bands near 2917 and 2849 cm^{-1} are the stretching vibrations of N–H in aliphatic structures and C–H in alkanes, aldehydes, and a carboxylic acid. The band near 1734 cm^{-1} is the stretching vibration of C=O in aldehydes. The peak of 1594 cm^{-1} is stretching C-O and C=C, resulting from ester, carbonyl, and carboxyl groups. The peaks between 1500 and 500 cm^{-1} are called the fingerprint region, representing a complex set of absorptions unique to each compound in the spectrum. It is described with the help of references instead of interpreting the peaks visually. As can be seen in Fig. 1, lignocellulosic adsorbent illustrated different peaks around 1374, 1027, and 581 cm^{-1}. These bands can generally be linked with the stretching vibrations of aromatic ester, amine, ester, and alkene groups, and $-NO_2$, $-CH_3$, CH_2, -CH, and C=O functional groups

were detected at these peaks. It can be concluded that these functional groups were mainly involved in the adsorption process considering the FTIR analysis.

The SEM–EDS image of the adsorbent is depicted in Fig. 2. As can be seen from the SEM images, a lignocellulosic form of the peel consists of many heterogeneous pore structures, allowing for adsorbing of zinc ions easily. The EDS analysis was also carried out to observe the elemental distribution of the biosorbent. The EDS results highlighted the C and O values in the peel were high (Fig. 2). Furthermore, the active sides, large surface, and dispersed porous on the peel make it possible to bind zinc ions.

3.2 The Contact Time, pH, and Adsorbent Dosage Effect

3.2.1 Contact Time

The contact time for reducing Zn^{2+} with banana peel is illustrated in Fig. 3. As shown in Fig. 3a, the sorption between lignocellulose and Zn^{2+} increased sharply in the first 10 min of contact time. The maximum removal happened within the 20 min contact time and then slightly changed, and equilibrium was reached in about 30 min. The removal rate was fast at the first 30 min, achieving 77% efficiency, and then no significant change in efficiency was observed because the process reached saturation (see Fig. 3). It can be explained the fact that there are more active sites on the peel at the beginning, resulting in rapid binding of zinc ions on the adsorbent and then followed by a decrease in the zinc removal rate with a decrease in the active site.

3.2.2 The pH Effect

The pH of the solution is important due to effecting zinc ionization ability and adsorbent surface characteristics (Y. Liu et al., 2019). The effects of pH on the reduction of Zn^{2+} were carried out. The results are demonstrated in Fig. 3. The reduction efficiency of Zn^{2+} increased with increasing pH value from 3.0 to 6.0. However, the removal rate remained stable, with pH values increasing until 10.0.

Divalent zinc ion in aqueous solution can be found at pH varying 1.0 to 6.0 considering The Atlas of Eh- pH Diagrams ("The Atlas of Eh- pH Diagrams" n.d.). Furthermore, a negative surface charge on the peel happened with high pH values.

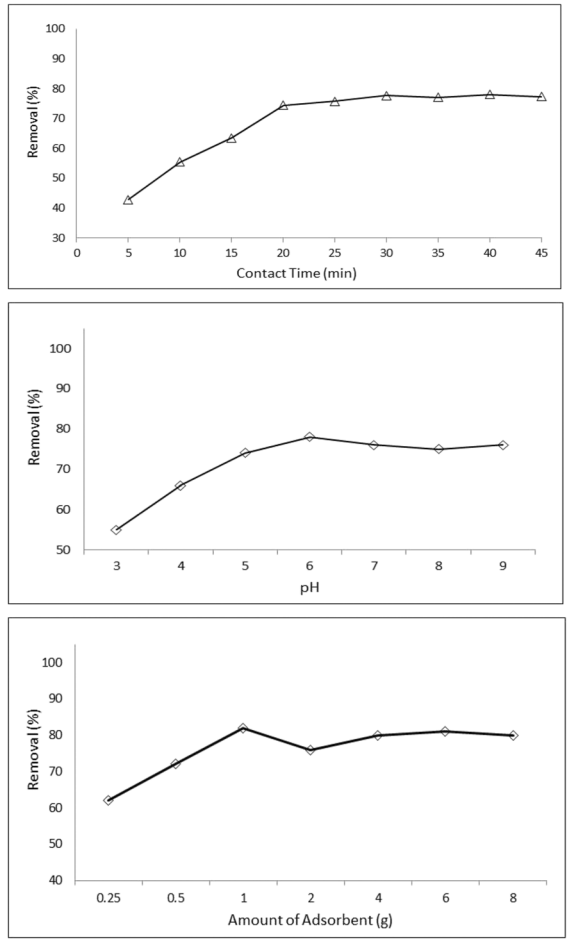

Fig. 3 Effect of contact time, pH, and adsorbent dosage on removal of zinc

The lover pH reduces the electrostatic repulsive force (Liu et al., 2019). The neutral pH was desirable for the absorption of Zn^{2+} due to high H^+ ions, occupation of the existing bonding site of peel, and obstructed Zn^{2+} adsorption on the peel. In other words, moreover, the HO^- is dominant bigger than that of pH value 6.0 and dual competition occurred for the active sites between anions and metals, concluded in a low reducing rate. The maximum removal rate was obtained at pH 6.0. It is most likely that the positively charged active groups on adsorbent repulse to Zn^{2+} ions. Furthermore, the chelation and the formation of metal hydroxide occur with increasing pH, enhancing the removal of zinc. These results are in line with the previous research (Depci et al., 2012) which informed that

maximum removal of zinc by using apple pulp and barley straw was achieved pH values 6.0 and 5.0, respectively.

3.2.3 Adsorbent Dosage

Figure 3 illustrates the adsorbent dose effect on zinc removal efficiency. The peel dose was increased from 0.25 g to 8.0 g at fixed pH and room temperature to determine the specification of a sorbent capacity. The removal rate of Zn^{2+} increased significantly from 62 to 82% due to the number of functional groups increase with increase sorbent dose, resulted in zinc reduction efficiency. The peel dose increases from 0.25 to 1.0 g, which increases the removal efficiency, and then goes on steadily. It can be explained by the fact that adsorbent saturation after sufficient ions are captured, and therefore the peel cannot further uptake Zn^{2+} (Liu et al., 2019). The maximum Zn^{2+} removal efficiency was 82%, and the optimum biosorbent amount of 1.0 g was used to obtain that of the percentage. In the batch adsorption experiments, the amount of adsorbent 1.0 g was chosen in terms of maximum removal efficiency. Previous researchers pointed out that the adsorbent dose, pH, and contact time significantly impact the removal efficiency.

3.3 Adsorption Isotherms and Kinetics

The equilibrium isotherm is applied to describe the sorbate and adsorbent interaction, and also the adsorption process is defined with the help of kinetic models. As commonly used isotherm models, Freundlich (Freundlich, 1906), Langmuir (Langmuir, 1918), and Dubinin-Radushkevich (Dubinin & Radushkevich, 1947) were applied the batch experiment data. Furthermore, the Lagergren pseudo–first-order (Lagergren, 1898) and the pseudo–second-order models (Ho & McKay, 1999) and the intra-particle diffusion model (Weber & Morris, 1963) were also applied to analyze the adsorption process, diffusion rate, and removal mechanism of Zn^{2+}. Isotherm and kinetic linearized form of equations, parameters, and correlation coefficients is given in Table 1.

3.3.1 Adsorption Isotherm

The Langmuir adsorption model is generally applied to describe the monolayer adsorption on the homogenous surfaces, which imply one active site is occupied by only one binding ion. The Langmuir constant (RL) gives information about the affinity of the sorbent for the binding ions. The constant is valued $RL > 1$, $RL = 1$, and $0 < RL < 1$; if $RL = 0$, the adsorption is undesirable, linear, desirable, and irreversible, respectively (Langmuir, 1918). The value of RL for the peel was 0.2289 which confirms the adsorption was desirable.

Contrary to the Langmuir model, the Freundlich model refers to heterogeneous adsorption having different energies of sorption, and there is no limit to the formation of monolayer (Freundlich, 1906). The Freundlich isotherm constant (1/n) is related to sorption intensity and the heterogeneity of the sorption process. The constant is valued as follows: $1/n = 0$ is irreversible process, $0 < 1/n < 1$ is favorable adsorption, and $1/n > 1$ unfavorable or cooperative adsorption. This model highlighted that active sites decrease as the ion binding increases, so the stronger binding sites are firstly used (Fernández-López et al., 2019). The Freundlich isotherm constant was 0.9095, referring to the favorable adsorption process and the removal of zinc that occurred on the heterogeneous surfaces by multi-layer adsorption.

The comparison of the experimental values and the predicted amount of equilibrium for banana peel is illustrated in Fig. 4. The calculated value of Langmuir isotherm is close to the experimental data, and the values of ARE, NSD, and MPSD error analysis are well fit to Langmuir isotherm which provides a better fit for the reduction of Zn^{2+}(see Table 1).

The Dubinin-Radushkevich isotherm is used to define the adsorption mechanism and nature using

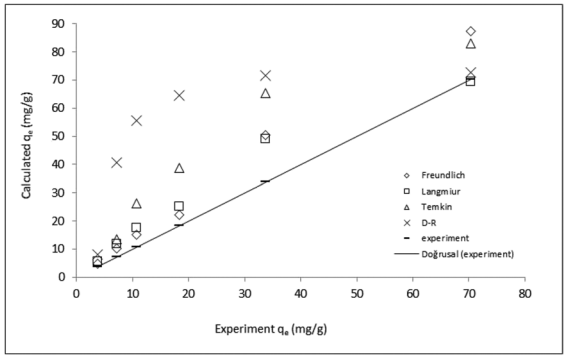

Fig. 4 The predicted amount of adsorption at equilibrium and the experimental values

a Gaussian energy distribution onto a heterogeneous surface. The effect of the porous structure can be described by the D–R equation model. The D–R isotherm average free energy (E) ranges from 1 to 8 $kJmol^{-1}$, and 9 to 16 kJ/mol indicates for physical and chemical sorption, respectively (Saltali et al., 2007). The (E) value was calculated as follows: 6.96 $kJmol^{-1}$. The result indicated that physical adsorption took place for the reduction of zinc ions from an aqueous solution. However, the correlation coefficient (R^2) demonstrated that D–R model application for the banana peel in this study is limited (see Table 1).

3.3.2 *Kinetic Study*

Heterogeneity of organic adsorbent surface makes complex the metal removal from an aqueous solution. The adsorption rate was the leading solid–liquid interface and affected by retention time (Kayranli, 2011). The pseudo–first-order model is applied to describe the equilibrium between the liquid and solid phase or the reversible reactions. On the other hand, the pseudo–second-order model defines the concentration of one second or two primary reactants (Ho & McKay, 1999). The pseudo–second-order model can more favorably define the zinc removal with the higher correlation coefficient ($R^2 > 0.96$), and the adsorption capacity value is also more close to the experimental result (Table 1). Researchers (Lee & Choi, 2018) informed that pseudo–second order is more applicable than pseudo–first order to analyze the sorption rate of most sorbents. The present findings comply with previous studies.

It is known a close link between the active sides and metal complexation in the adsorbent process. As seen in Fig. 5, the intra-particle diffusion plot was not linear. The plot can be divided into three linear regions, demonstrating adsorption was governed by more than one mechanism, external/film diffusion, internal particle diffusion, and both film and intra-particle diffusions. The internal particle diffusion rate constant was 9.39 mg/g/ $min^{1/2}$. The result demonstrated that the intra-particle diffusion and other mechanisms governed the zinc removal process considering the multi-linearity of the plots and boundary layer thickness. Furthermore, intra-particle diffusion and surface adsorption co-occurred. Ho and McKay (2003) highlighted that the rate-limiting step in the adsorption process could be chemical reaction

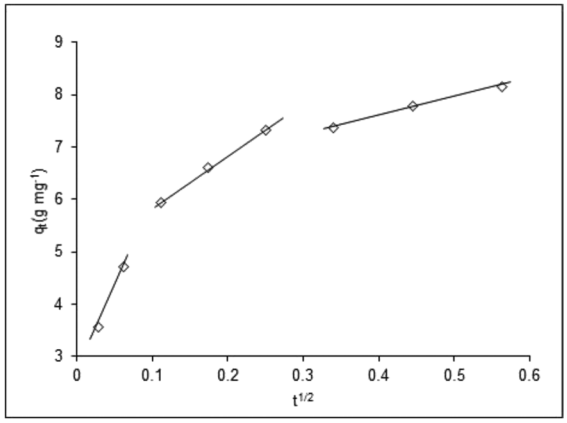

Fig. 5 Intra-particle diffusion curve

mechanisms like sharing or exchanging the electrons between adsorbents.

4 Possible Zinc Sorption Mechanisms

Fruit residuals are used as low-priced and eco-friendly biosorbents to reduce metals from an aqueous solution. Previous researchers studied metal ion reduction with the adsorption process; however, there is no detailed explanation of the interaction mechanisms due to the complex chemical composition and multiple mechanisms. The metal adsorption behavior depends on the pH solution, chemistry of metal, and binding characteristics of lignocellulose. Furthermore, interaction mechanisms are extensively related to chemical structure, surface area, and active groups (–COOH, –OH, $–CH_3$, $–NO_2$, $–CH_2$, –CH, C-H, C-O, C-N) of the used sorbents. The main removal mechanisms are ion exchange, metal complexation, physical/chemical adsorption, chelation, chemical/surface precipitation, and intra-particle diffusion (Kaur et al., 2020; Trakal et al., 2016). However, the reduction mechanism of zinc in the sorption process consists of complex and challenging to understand steps.

As can be explained in Sect. 3.1, banana peel is composed of very rich chemical compositions such as lignin, cellulose, and hemicellulose. Also, other components are lipids, proteins, simple sugars, and ash, having a different ratio. The used sorbent includes more functional groups on the surface governing the adsorption process. The interaction mechanism's specific role depends on functional

groups of biosorbent, metal ionizations, and aqueous environments (Lv et al., 2018).

pH is the critical parameter in an adsorption process because of its effect on the metal ion ionization degree and solubility, and the active groups of the sorbents. The adsorption rate of many cationic metal ions is very high at a pH value of 5.0–6.0. The physical adsorption is generated by functional groups, heterogeneity, and polarity of adsorbent via electrostatic attraction and ion–dipole forces (Yang et al., 2019). The hydroxyl groups derived from cellulose and hemicellulose play a role in the binding of zinc ions. Similarly, the carboxyl groups form of -COO^- under a particular pH provide reducing the cationic metal efficiently (Ali et al., 2016). Many polar groups on the sorbent, which a certain amount of zinc ions can occupy to form an electric double layer, resulted in zeta potential. Positively charged ions were captured easily through the peel's increase of negative surface charge (Ni et al., 2019).

The electrostatic interaction is generated with the help of divalent metals and negatively charged functional groups on the sorbent. The lignocellulosic sorbent is represented by B, and the protonation equilibria for the amino group, $–NO_2$, and the hydroxyl of C-6, –OH, is as follows;

$$B - O - NO_2 + H^+ \rightarrow HO - B - NO_2$$
$$H_{-1}B + H \rightarrow B$$
$$B - HO - NO_2 + H^+ \rightarrow O - S - NO_3{}^+H_2O$$
$$B + H \rightarrow HS$$

where $H_{-1}S$ is the completely deprotonated unit, the dimeric shell unit with C-6 hydroxyl group protonated, and HS the protonated sites.

The other main zinc removal process is ion exchange, taking place with the availability of carboxyl and hydroxyl functional groups which include oxygen. The functional group chemistry and metal ion size affect the process efficiency (Yang et al., 2019). Specifically, an acidic functional group plays a critical role in the removal of heavy metals by organic adsorbents. The zinc removal rate increased at pH 6.0 due to a negative adsorption surface increase. NH_4OH was used for the pH adjustments, resulting in hydroxide forming the $Zn(HO)_2$ salt. The removal efficiency was affected by pH, concluding one of the adsorption mechanisms is cation exchange (Ali et al., 2016). Hu et al. (2017) informed that metal hydroxide form is generated in solution at neutral pH or alkaline conditions, and metal hydroxyl salt precipitates out in aqueous. In the present study, the pH buffering agent was NH_4OH that provides the formation of the metal carboxylate with the exchange of divalent metal with the proton in the carboxyl groups. The ion exchange process is given below equations:

$$RCOOH + NH_4OH \rightarrow RCOONH_4 + H_2O,$$
$$2RCOOHNH_4 + ZnCl_1 \rightarrow 2RCOOZn + NH_4Cl$$
$$B - OH + Zn^{2+} \rightarrow B - O - Zn^+ + 2H^+$$
$$B - NO_2 + Zn^{2+} \rightarrow B - NO - Zn^+ + H_2O^+$$
$$B - COOH + Zn^{2+} \rightarrow B - COO - Zn^+ + 2H^+$$

The salt reaction is mostly as follows;

$$B - OH + Zn(OH)_2 \rightarrow B - O - ZnOH + H_2O$$
$$B - NO_2 + Zn(OH)_2 \rightarrow B - NO - ZnOH$$

Surface complexations are also important to process in sorption taking place with multi-atom structures and metal-functional group interaction. The active group (carboxyl/carbonyl) binds zinc, resulting in a complexation (Peng et al., 2017). Ali et al. (2016) highlighted that chemical adsorption may be the rate-controlling step due to forming chemical bonds with exchange or sharing electrons between sorbent and sorbate in process. The following equations can define the formation of complex species;

$$B + Zn^{2+} \rightarrow BZn^{2+}$$
$$Zn^{2+} + B + H \rightarrow BHZn^{2+}$$
$$Zn^{2+} + B + OH \rightarrow Zn^{2+}BOH$$

Fernández-López et al. (2019) highlighted that sorption kinetic models help to define the chemical/physical reaction, and diffusion, the proper reaction rate. Furthermore, Ho and McKay (2003) informed that chemisorption could be the rate-limiting step through the adsorption process because electrons exchange or share between sorbent and sorbate occurred. The pseudo–second-order equation described well for the zinc capturing with banana peel considering both validity and correlation coefficients (see Table 1). It can be concluded that the sorption process is the adsorption-complex interactions through electron exchange or sharing.

The intra-particle diffusion model provided valuable information related to zinc ion diffusion to the adsorbent due to the porous structure of the shells. As

seen in Fig. 5, the intra-particle plot can be categorized into three linear regions; the first plot refers to the external surface and the fastest due to the existence of more binding sites, the second is the intra-particle diffusion and the gradual adsorption stage, and the final is the lowest and represents the intra-particle or both film and intra-particle diffusions because low zinc ions remained in solution. These finding also shows that sorption was governed by more than one mechanism, external/film diffusion, internal particle diffusion, and both film and intra-particle diffusions.

SEM–EDS image helps to explain the adsorption interaction between Zn^{2+} ions and bioadsorbent (in Fig. 2). As shown in Fig. 2, the lignocellulosic adsorbent has layered structures, and the C and O values at the peel are high. The peel comprises rough surfaces and a significant number of heterogeneous porous layers, enabling the sorbent to capture zinc ions effectively. After sorption, these layers and rough surfaces were occupied with zinc ions, which resulted in flatting. Sphere structures have been formed on the surface layer due to zinc ions' bond to the surface. Similarly, FTIR spectra of the biosorbent showed that functional groups of hydroxyl and carbonyl/carboxyl play important roles in the adsorption of zinc, and the adsorption increases over time. Furthermore, this adsorption resulted in changing the peaks and transmittances (see Fig. 1 and Table 2).

As seen in Fig. 1, the peak at 3293 cm^{-1} is a large band, and the number of hydroxyl and carboxyl groups shifted finally 3341 cm^{-1} upon Zn^{2+} adsorption. The spectra analysis of the biosorbent during the reducing process demonstrated the peak transmittance changed from 45.0 to 35.0.0% (2971 cm^{-1}) for aliphatic structures and alkanes; 2849 cm^{-1} assigned for ester, carboxyl groups, and alkene (C-H) transmittance decrease from 54.0 to 47.0%; 1734 cm^{-1} assigned for C = O aldehyde transmittance altered from 78.0 to 69.0%. Similarly, the carboxyl/carbonyl group and ester band shifted from 1594 to 1607 cm^{-1} end of the process. These findings imply that there is interaction between the hydroxyl/carboxyl groups and Zn^{2+} ions. The peak between 1500 and 500 cm^{-1} is called fingerprint regions, and the absorption bands in this region, on the other hand, cause the entire molecule to vibrate rather than individual functional groups. The peak 1442 cm^{-1} came out after the sorption process, referring to the alkene. The band at 1374 cm^{-1} indicates $-NO_2$, $-CH_3$, $-CH_2$, -CH groups produced from lignin, cellulose, hemicellulose, and the transmittance decreased 3.0%. The peak near 1315, 1242, and 886 cm^{-1} is the stretching vibration of aromatic ester (C-O), amine (C-N), and alkanes (C = C, C–H), observed after the sorption process, respectively. The other peak change was seen 1027, and 581 cm^{-1} represents ester and carboxyl groups.

As seen in Table 1 and Fig. 1, the transmittance and peak shifts informed that the active sites on the absorbent, O–H, C–C, C-N, C = O, C = C, N–H, NO_2, $-CH_3$,—CH_2, and -CH functional group mainly were taken part in the adsorption process. These changes

Table 2 Banana peel functional groups, IR peak, and transmittance change in the process

Before adsorption		After adsorption		Assignment
IR peak	Transmittance %	IR peak	Transmittance%	
3293	47.0	3341	52.0	O–H, C-H (hydroxyl, carboxyl acid groups)
2917	45.0	2917	35.0	N–H (aliphatic structures, alkane)
2849	54.0	2849	47.0	C-H (ester, carboxyl groups, alkene)
1734	78.0	1734	69.0	C = O (Aldehyde)
1594	64.0	1607	64.0	C-O, C = C (ester, carbonyl, carboxyl groups)
-	-	1442	68.0	C-H (Alkane)
1374	65.0	1374	62.0	$-NO_2$, $-CH_3$, $-CH_2$, -CH groups
-	-	1315	68.0	C-O (Aromatic ester)
-	-	1242	70.0	C-N (Amine)
1027	48.5	1026	48.0	C = O (ester, carboxyl groups)
-	-	886	74.0	C = C, C-H (alkene)
581	72.0	557	70.0	C = O (ester, carboxyl groups)

could be explained by the complex interaction mechanism of adsorbent and adsorbate. Furthermore, experimental factors also affect the chemistry and physical properties of biosorbent, and pH affects both sorbent surface and zinc ionizations. Furthermore, experimental factors also affect biosorbent chemistry, and physical properties such as pH affect both sorbent surface charge and zinc ionizations. The mechanism of Zn^{2+} adsorption by banana peel can be likely that the ions firstly bond sorbent with chemical interaction, via the carboxyl-carbonyl groups on the biosorbent surface, and then, multilayer adsorption as a film covering the adsorbent surface occurred (Huang et al., 2018). As seen in Fig. 6, different removal mechanisms such as the electrostatic interaction, ion exchange, electrostatic complexation, functional groups, and co-precipitation/inner-sphere complexation occur for the sequestration of zinc.

5 Adsorption Capacity Comparison

A comparison of banana skin capacity with other organic adsorbents was performed to determine the peel's applicability for the Zn^{2+} removal process (see Table 3). The availability of active sites affects the metal-binding capacity of adsorbents. The different experimental conditions and chemical and physical characteristics of the biosorbent make the direct comparison difficult. However, the finding showed that the Zn^{2+} adsorption capacity of banana peel is higher than the recently used adsorbent reported in Table 3. Liu et al. (2012) and Feizi and Jalali (2015) informed that the Zn^{2+} removal rate for watermelon rind and the walnut shell is 6.845 mg/g and 33.3 mg/g. Similarly, Çoruh et al. (2014) used an activated almond shell to reduce zinc from aqueous solution and reported a maximum adsorption capacity of 5.54 mg/g. Furthermore, the previous researchers carried out zinc removal by using organic adsorbent and informed that adsorption capacity of pecan shell is 17.21 mg/g (Segovia-Sandoval et al., 2018), modified pecan shell 27.86 mg/g (Segovia-Sandoval et al., 2018), spent coffee grounds 2.25 mg/g (Futalan et al., 2019), and apple pulp 11.72 mg/g (Depci et al., 2012). The maximum adsorption capacity of banana skin was higher than that of spent coffee ground, apple pulp, and almond shell. As seen in Table 3, the

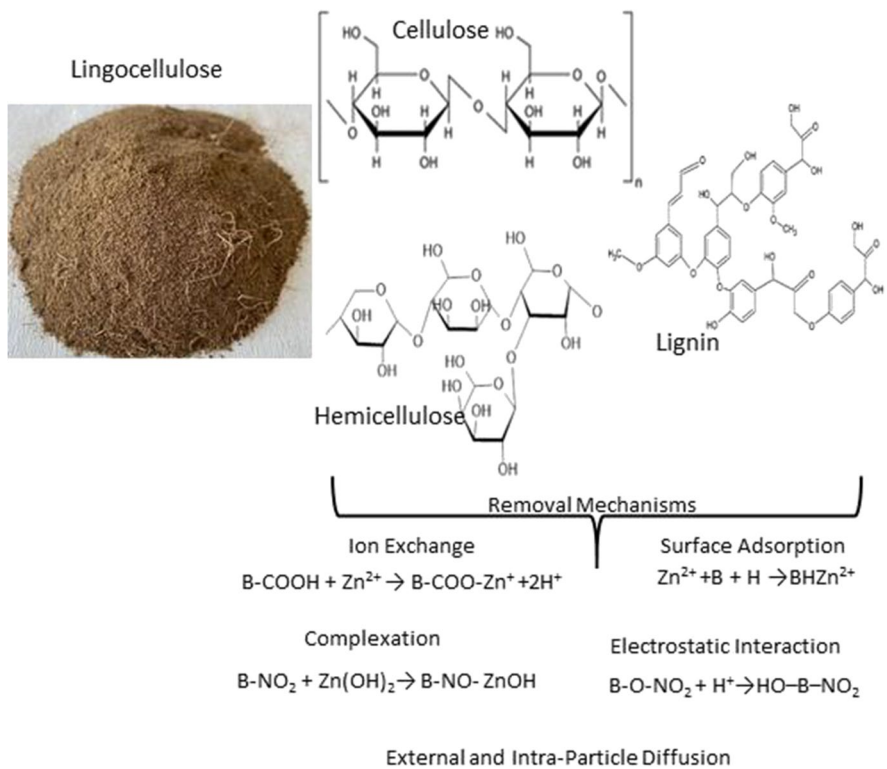

Fig. 6 Possible adsorption mechanisms of Zn^{+2}

Table 3 Comparison studies of banana peel

Organic adsorbent	Isotherm/kinetic models	Adsorption capacity (mg/g)	References
Watermelon rind	Langmuir/pseudo–second order	6.845	(Liu et al., 2012)
Walnut shells	Langmuir/pseudo–second order	33.3	(Feizi & Jalali, 2015)
Pecan shells	Prausnitz-Radke/n/a	17.21	(Segovia-Sandoval et al., 2018)
Modified pecan shells	Prausnitz-Radke/n/a	27.86	(Segovia-Sandoval et al., 2018)
Spent coffee grounds	Erlich/pusedo-second order	5.25	(Futalan et al., 2019)
Activated almond shell	Freundlich/n/a	5.54	(Çoruh et al., 2014)
Apple pulp	Langmuir/pseudo–second order	11.72	(Depci et al., 2012)
Spent coffee grounds	Langmuir/pseudo–second order	19.4–22.3	(Chwastowski et al., 2020)
Banana peels	Langmuir/pseudo–second order	92.59	This study

peel can be used as a low-priced and efficient adsorbent for the adsorption of zinc ions.

6 The Usage of Zinc-Enriched Banana Peel as a Soil Conditioner

Chemical fertilizers are used for the increased yield in many years. The usage of the chemical fertilizer contributes to the growth of plants, however, not helping to improve the soil characteristic. On the other hand, there is a growing interest in using bio-organic fertilizer/conditioner instead of chemical fertilizers due to high costs, contamination, and inappropriate application causing soil quality degradation (Omoni et al., 2020). The world trend is that while soil biodiversity is protected, quality crops concerning sustainability are produced. Organic fertilizers are cheap nutrient sources and enhance crop production in low-input agriculture.

Banana peel is mainly used to improve the soil physicochemical and microbiological characteristics and enhance plant productivity. Anastopoulos et al. (2019) pointed out that the availability of banana peel in soil has an important effect on the microbial community due to the contents of organic compounds and minerals. Furthermore, the peel supports the formation of a clay-humic complex and decreases the permeability resulting in increased water holding capacity of the soil. The banana peel is composed of nutritious minerals, mostly potassium (K), sodium (Na), calcium (Ca), and manganese (Mn) (Lobo & Dorta, 2019). Banana peel, as an alternative potassium source, could be used as a potassium fertilizer for plant productivity due to its high potassium contents. Increasing soil alkalinity and changing the soil anions capacity are beneficial for plants' growth. Potassium is also enhancing plant resistance to pests, diseases, and abiotic stresses. It needs to activate more than 80 different enzymes responsible for plant and animal processes such as starch synthesis, nitrate reduction, energy metabolism, and photosynthesis (Islam et al., 2019).

Zinc is an essential micronutrient for most physiological processes. The potential phytotoxicity at leaf tissue occurs possibly lower than concentrations above 0.2 mg/g dry matter (Tsonev & Lidon, 2012). Phytotoxicity causes a decrease in yield and, photosynthetic performance as photochemical reactions, carbonic anhydrase activity. The soil pH affects the availability of major nutrients concentrations, the microelements for plant uptake, and also total Zn concentration and activity in soil solution. The high pH reduces the total Zn concentration and activity. Calcareous soil results in weak soil–plant productivity due to lack of nutrients, especially N, P, micronutrients, and soil organic matter. Bio-organic conditioners help to improve nutrient losses and enhance plant growth in calcareous soil (Hafez et al., 2021).

The banana peel contains organic materials, nutrients, and minerals, and then holding zinc with functional groups makes it a valuable soil conditioner/amendment. The composition and concentration of the plant growth media effects zinc uptake by the plants depending on plant species. The ideal soil pH for plant growth is between 6.0 and 8.0, called neutral soil. The end-product pH for the adsorption process is 6.0. The end-product can also be used for reducing the pH of the alkaline and high alkaline soil ($pH > 8$).

7 Conclusion

The lignocellulosic adsorbent was characterized by FTIR spectra, SEM–EDS images, and elemental analysis. The effect of contact time, pH, and adsorbent dosage on the sequestration of zinc was observed. This research showed that banana peel is an effective eco-friendly, low-cost adsorbent for removing Zn^{2+} from aqueous solutions. Langmuir isotherm and the pseudo–second-order kinetic model have well described the banana peel adsorption. The peel adsorption capacity is 59.52 mg/g. The kinetic experiment results demonstrated the rate-controlling sorption for Zn^{2+} only was not the intra-particle diffusion. Active groups on the peel surface can incorporate zinc ions in many ways, electrostatic interaction, physical adsorption, ion exchange, and surface complexation. The by-product of this study can also be used to reduce the soil pH, especially for alkaline and high alkaline soil (pH > 8). Furthermore, the end-product is composed of organic compounds with zinc that can be used as a soil amendment for sustainable agriculture, resulting in reducing the disposal cost of the end-products for sustainable environmental management. Further research including soil conditioner water holding capacity, microorganism activity, effect on the plant growth, and release zinc to soil should be studied.

Data Availability The datasets used and/or analyzed during the current study are available from the corresponding author on reasonable request.

Declarations

Competing Interests The authors declare no competing interests.

References

Ali, R. M., Hamad, H. A., Hussein, M. M., & Malash, G. F. (2016). Potential of using green adsorbent of heavy metal removal from aqueous solutions: Adsorption kinetics, isotherm, thermodynamic, mechanism and economic analysis. *Ecological Engineering, 91*, 317–332. https://doi.org/10.1016/j.ecoleng.2016.03.015

Anastopoulos, I., Omirou, M., Stephanou, C., Oulas, A., Vasiliades, M. A., Efstathiou, A. M., & Ioannides, I. M. (2019). Valorization of agricultural wastes could improve soil fertility and mitigate soil direct N2O emissions. *Journal of Environmental Management, 250*, 109389. https://doi.org/10.1016/j.jenvman.2019.109389

Baloo, L., Isa, M. H., Sapari, N. B., Jagaba, A. H., Wei, L. J., Yavari, S., et al. (2021). Adsorptive removal of methylene blue and acid orange 10 dyes from aqueous solutions using oil palm wastes-derived activated carbons. *Alexandria Engineering Journal, 60*(6), 5611–5629. https://doi.org/10.1016/j.aej.2021.04.044

Chwastowski, J., Bradło, D., & Żukowski, W. (2020). Adsorption of cadmium, manganese and lead ions from aqueous solutions using spent coffee grounds and biochar produced by its pyrolysis in the fluidized bed reactor. *Materials, 13*(12), 1–14. https://doi.org/10.3390/ma13122782

Çoruh, S., Geyikçi, F., Kiliç, E., & Çoruh, U. (2014). The use of NARX neural network for modeling of adsorption of zinc ions using activated almond shell as a potential biosorbent. *Bioresource Technology, 151*, 406–410. https://doi.org/10.1016/j.biortech.2013.10.019

Costa, H. P. de S., da Silva, M. G. C., & Vieira, M. G. A. (2021, April 1). Biosorption of aluminum ions from aqueous solutions using non-conventional low-cost materials: A review. *Journal of Water Process Engineering*. Elsevier Ltd. https://doi.org/10.1016/j.jwpe.2021.101925

Depci, T., Kul, A. R., & Önal, Y. (2012). Competitive adsorption of lead and zinc from aqueous solution on activated carbon prepared from Van apple pulp: Study in single- and multi-solute systems. *Chemical Engineering Journal, 200–202*, 224–236. https://doi.org/10.1016/j.cej.2012.06.077

Dimkpa, C. O., Andrews, J., Sanabria, J., Bindraban, P. S., Singh, U., Elmer, W. H., et al. (2020). Interactive effects of drought, organic fertilizer, and zinc oxide nanoscale and bulk particles on wheat performance and grain nutrient accumulation. *Science of the Total Environment, 722*, 137808. https://doi.org/10.1016/j.scitotenv.2020.137808

Dubinin, M. M., & Radushkevich, L. V. (1947). The equation of the characteristic curve of activated charcoal. *Proceedings of the Academy of Sciences, Physical Chemistry Section, 55*, 331–337.

FAOSTAT. http://www.fao.org/faostat/en/#data/QL

Feizi, M., & Jalali, M. (2015). Removal of heavy metals from aqueous solutions using sunflower, potato, canola and walnut shell residues. *Journal of the Taiwan Institute of Chemical Engineers, 54*, 125–136. https://doi.org/10.1016/j.jtice.2015.03.027

Fernández-López, J. A., Angosto, J. M., Roca, M. J., & Doval Miñarro, M. (2019). Taguchi design-based enhancement of heavy metals bioremoval by agroindustrial waste biomass from artichoke. *Science of the Total Environment, 653*, 55–63. https://doi.org/10.1016/j.scitotenv.2018.10.343

Futalan, C. M., Kimm, J.; Yee, J.-J. (2019). Adsorptive treatment via simultaneous removal of copper, lead and zinc from soil washing wastewater using spent coffee grounds. *Water Science and Technol Ogy, 79* (6), 1029-1041 https://doi.org/10.2166/wst.2019.087

Freundlich, H. M. F. (1906). Over the adsorption in solution. *The Journal of Physical Chemistry, 57*, 385–471.

Hafez, M., Popov, A. I., & Rashad, M. (2021). Environmental technology & ınnovation ıntegrated use of bio-organic

fertilizers for enhancing soil fertility – plant nutrition, germination status and initial growth of corn (Zea Mays L .). *Environmental Technology & Innovation*, *21*, 101329. https://doi.org/10.1016/j.eti.2020.101329

Ho, Y. S., & McKay, G. (1999). Pseudo-second order model for sorption processes. *Process Biochemistry, 34*(5), 451–465. https://doi.org/10.1016/S0032-9592(98)00112-5

Ho, Y. S., & McKay, G. (2003). Sorption of dyes and copper ions onto biosorbents. *Process Biochemistry, 38*(7), 1047–1061. https://doi.org/10.1016/S0032-9592(02)00239-X

Hu, C., Zhu, P., Cai, M., Hu, H., & Fu, Q. (2017). Comparative adsorption of Pb(II), Cu(II) and Cd(II) on chitosan saturated montmorillonite: Kinetic, thermodynamic and equilibrium studies. *Applied Clay Science, 143*, 320–326. https://doi.org/10.1016/j.clay.2017.04.005

Hu, W., Jiang, N., Yang, J., Meng, Y., Wang, Y., Chen, B., et al. (2016). Potassium (K) supply affects K accumulation and photosynthetic physiology in two cotton (Gossypium hirsutum L.) cultivars with different K sensitivities. *Field Crops Research, 196*, 51–63. https://doi.org/10.1016/j.fcr.2016.06.005

Huang, F., Gao, L.-Y., Deng, J.-H., Chen, S.-H., & Cai, K.-Z. (2018). Quantitative contribution of Cd^{2+} adsorption mechanisms by chicken-manure-derived biochars. *Environmental Science and Pollution Research, 25*, 28322–28334. https://doi.org/10.1007/s11356-018-2889-y

Langmuir, I. (1918). Adsorption of gases on plain surfaces of glass, mica and platinum. *Journal of the American Chemical Society, 40*, 1361–1403.

Islam, M., Halder, M., Siddique, M. A. B., Razir, S. A. A., Sikder, S., & Joardar, J. C. (2019). Banana peel biochar as alternative source of potassium for plant productivity and sustainable agriculture. *International Journal of Recycling of Organic Waste in Agriculture, 8*(s1), 407–413. https://doi.org/10.1007/s40093-019-00313-8

Jagaba, A. H., Kutty, S. R. M., Hayder, G., Baloo, L., Ghaleb, A. A. S., Lawal, I. M., et al. (2021). Degradation of Cd, Cu, Fe, Mn, Pb and Zn by Moringa-oleifera, zeolite, ferric-chloride, chitosan and alum in an industrial effluent. *Ain Shams Engineering Journal, 12*(1), 57–64. https://doi.org/10.1016/j.asej.2020.06.016

Jagaba, A. H., Kutty, S. R. M., Khaw, S. G., Lai, C. L., Isa, M. H., Baloo, L., et al. (2020). Derived hybrid biosorbent for zinc(II) removal from aqueous solution by continuous-flow activated sludge system. *Journal of Water Process Engineering, 34*, 101152. https://doi.org/10.1016/j.jwpe.2020.101152

Kaur, M., Kumari, S., & Sharma, P. (2020). Removal of Pb (II) from aqueous solution using nanoadsorbent of Oryza sativa husk: Isotherm, kinetic and thermodynamic studies. *Biotechnology Reports, 25*, e00410. https://doi.org/10.1016/j.btre.2019.e00410

Kayranli, B. (2011). Adsorption of textile dyes onto iron based waterworks sludge from aqueous solution; isotherm, kinetic and thermodynamic study. *Chemical Engineering Journal, 173*(3), 782–791. https://doi.org/10.1016/j.cej.2011.08.051

Lagergren, S. (1898). *About the theory of so-called adsorption of soluble substances*. Kungliga Svenska Vetenskapsakademiens Handlingar.

Lee, S. Y., & Choi, H. J. (2018). Persimmon leaf bio-waste for adsorptive removal of heavy metals from aqueous solution. *Journal of Environmental Management, 209*, 382–392. https://doi.org/10.1016/j.jenvman.2017.12.080

Li, C., Ji, G., Qu, Y., Irfan, M., Zhu, K., Wang, X., & Li, A. (2021a). Influencing mechanism of zinc mineral contamination on pyrolysis kinetic and product characteristics of corn biomass. *Journal of Environmental Management, 281*, 111837. https://doi.org/10.1016/j.jenvman.2020.111837

Li, Z., Gong, Y., Zhao, D., Dang, Z., & Lin, Z. (2021b). Enhanced removal of zinc and cadmium from water using carboxymethyl cellulose-bridged chlorapatite nanoparticles. *Chemosphere, 263*, 128038. https://doi.org/10.1016/j.chemosphere.2020.128038

Liew, L. C., Katsuda, T., Gailhouste, L., Nakagama, H., & Ochiya, T. (2017). Mesenchymal stem cell-derived extracellular vesicles: A glimmer of hope in treating Alzheimer's disease. *International Immunology, 29*(1), 11–19. https://doi.org/10.1093/intimm/dxx002

Liu, C., Ngo, H. H., & Guo, W. (2012). Watermelon rind: Agro-waste or superior biosorbent? *Applied Biochemistry and Biotechnology, 167*(6), 1699–1715. https://doi.org/10.1007/s12010-011-9521-7

Liu, Y., Gao, Q., Pu, S., Wang, H., Xia, K., Han, B., & Zhou, C. (2019). Carboxyl-functionalized lotus seedpod: A highly efficient and reusable agricultural waste-based adsorbent for removal of toxic Pb 2+ ions from aqueous solution. *Colloids and Surfaces A: Physicochemical and Engineering Aspects, 568*, 391–401. https://doi.org/10.1016/j.colsurfa.2019.02.017

Lobo, M. G., & Dorta, E. (2019). Utilization and management of horticultural waste. In *Postharvest Technology of Perishable Horticultural Commodities* (pp. 639–666). Elsevier. https://doi.org/10.1016/B978-0-12-813276-0.00019-5

Lonergan, Z. R., & Skaar, E. P. (2019, December 1). Nutrient zinc at the host–pathogen ınterface. *Trends in Biochemical Sciences*. Elsevier Ltd. https://doi.org/10.1016/j.tibs.2019.06.010

Lv, D., Liu, Y., Zhou, J., Yang, K., Lou, Z., Baig, S. A., & Xu, X. (2018). Application of EDTA-functionalized bamboo activated carbon (BAC) for Pb(II) and Cu(II) removal from aqueous solutions. *Applied Surface Science, 428*, 648–658. https://doi.org/10.1016/j.apsusc.2017.09.151

Ni, B. J., Huang, Q. S., Wang, C., Ni, T. Y., Sun, J., & Wei, W. (2019). Competitive adsorption of heavy metals in aqueous solution onto biochar derived from anaerobically digested sludge. *Chemosphere, 219*, 351–357. https://doi.org/10.1016/j.chemosphere.2018.12.053

Omoni, V. T., Lag-Brotons, A. J., & Semple, K. T. (2020). Impact of organic amendments on the development of 14C-phenanthrene catabolism in soil. *International Biodeterioration and Biodegradation, 151*, 104991. https://doi.org/10.1016/j.ibiod.2020.104991

Oosterhuis, D. M., Loka, D. A., Kawakami, E. M., & Pettigrew, W. T. (2014). The physiology of potassium in crop production. In *Advances in Agronomy* (Vol. 126, pp. 203–233). Academic Press Inc. https://doi.org/10.1016/B978-0-12-800132-5.00003-1

Parab, H., & Sudersanan, M. (2010). Engineering a lignocellulosic biosorbent - Coir pith for removal of cesium from aqueous solutions: Equilibrium and kinetic studies. *Water Research, 44*(3), 854–860. https://doi.org/10.1016/j.watres.2009.09.038

Peng, W., Li, H., Liu, Y., & Song, S. (2017, March 1). A review on heavy metal ıons adsorption from water by graphene oxide and its composites. *Journal of Molecular Liquids*. Elsevier B.V. https://doi.org/10.1016/j.molliq.2017.01.064

Saeed, A. A. H., Harun, N. Y., Sufian, S., Bilad, M. R., Nufida, B. A., Ismail, N. M., et al. (2021). Modeling and optimization of biochar based adsorbent derived from Kenaf using response surface methodology on adsorption of CD2+. *Water (Switzerland)*, *13*(7). https://doi.org/10.3390/w13070999

Saltali, K., Sari, A., & Aydin, M. (2007). Removal of ammonium ion from aqueous solution by natural Turkish (Yi{dotless}ldi{dotless}zeli) zeolite for environmental quality. *Journal of Hazardous Materials, 141*(1), 258–263. https://doi.org/10.1016/j.jhazmat.2006.06.124

Sanka, P. M., Rwiza, M. J., & Mtei, K. M. (2020). Removal of selected heavy metal ıons from ındustrial wastewater using rice and corn husk biochar. *Water, Air, and Soil Pollution*, *231*(5). https://doi.org/10.1007/s11270-020-04624-9

Sauer, S. (2018). Soy expansion into the agricultural frontiers of the Brazilian Amazon: The agribusiness economy and its social and environmental conflicts. *Land Use Policy, 79*, 326–338. https://doi.org/10.1016/j.landusepol.2018.08.030

Segovia-Sandoval, S. J., Ocampo-Pérez, R., Berber-Mendoza, M. S., Leyva-Ramos, R., Jacobo-Azuara, A., & Medellín-Castillo, N. A. (2018). Walnut shell treated with citric acid and its application as biosorbent in the removal of Zn(II). *Journal of Water Process Engineering, 25*, 45–53. https://doi.org/10.1016/j.jwpe.2018.06.007

Sial, T. A., Khan, M. N., Lan, Z., Kumbhar, F., Ying, Z., Zhang, J., et al. (2019). Contrasting effects of banana peels waste and its biochar on greenhouse gas emissions and soil biochemical properties. *Process Safety and Environmental Protection, 122*, 366–377. https://doi.org/10.1016/j.psep.2018.10.030

The Atlas of Eh- pH Diagrams. (n.d.).

Trakal, L., Veselská, V., Šafařík, I., Vítková, M., Číhalová, S., & Komárek, M. (2016). Lead and cadmium sorption mechanisms on magnetically modified biochars. *Bioresource Technology, 203*, 318–324. https://doi.org/10.1016/j.biortech.2015.12.056

Tsonev, T., & Lidon, F. J. C. (2012). Zinc in plants - An overview. *Emirates Journal of Food and Agriculture, 24*(4), 322–333.

Wang, X., Wang, J., Song, S., Rao, P., Wang, R., & Liu, S. (2020). Preparation and properties of soil conditioner microspheres based on self-assembled potassium alginate and chitosan. *International Journal of Biological Macromolecules, 147*, 877–889. https://doi.org/10.1016/j.ijbiomac.2019.09.247

Weber, W. J., & Morris, J. C. (1963). Kinetics of adsorption on carbon from solution. *Journal of the Sanitary Engineering Division, 81*, 31–60.

Xu, L., Cao, G., Xu, X., Liu, S., Duan, Z., He, C., et al. (2017). Simultaneous removal of cadmium, zinc and manganese using electrocoagulation: Influence of operating parameters and electrolyte nature. *Journal of Environmental Management, 204*, 394–403. https://doi.org/10.1016/j.jenvman.2017.09.020

Yang, X., Wan, Y., Zheng, Y., He, F., Yu, Z., Huang, J., et al. (2019, June 15). Surface functional groups of carbon-based adsorbents and their roles in the removal of heavy metals from aqueous solutions: A critical review. *Chemical Engineering Journal*. Elsevier B.V. https://doi.org/10.1016/j.cej.2019.02.119